Cell

ncRNA- and Pc2 Methylation-Dependent Gene Relocation between Nuclear Structures Mediates Gene Activation Programs

Liuqing Yang,[1,2,6] Chunru Lin,[1,2,6] Wen Liu,[1,3] Jie Zhang,[1] Kenneth A. Ohgi,[1] Jonathan D. Grinstein,[1,4] Pieter C. Dorrestein,[5] and Michael G. Rosenfeld[1,2,*]
[1]Howard Hughes Medical Institute
[2]Department of Medicine, Division of Endocrinology and Metabolism
[3]Graduate Program in Biology
[4]Graduate Program in Biomedical Sciences
[5]Skaggs School of Pharmacy and Pharmaceutical Sciences/Department of Chemistry and Biochemistry
University of California, San Diego, School of Medicine, 9500 Gilman Drive, La Jolla, CA 92093-0648, USA
[6]These authors contributed equally to this work
*Correspondence: mrosenfeld@ucsd.edu
DOI 10.1016/j.cell.2011.08.054

SUMMARY

Although eukaryotic nuclei contain distinct architectural structures associated with noncoding RNAs (ncRNAs), their potential relationship to regulated transcriptional programs remains poorly understood. Here, we report that methylation/demethylation of Polycomb 2 protein (Pc2) controls relocation of growth-control genes between Polycomb bodies (PcGs) and interchromatin granules (ICGs) in response to growth signals. This movement is the consequence of binding of methylated and unmethylated Pc2 to the ncRNAs *TUG1* and *MALAT1/NEAT2*, located in PcGs and ICGs, respectively. These ncRNAs mediate assembly of multiple corepressors/coactivators and can serve to switch mark recognition by "readers" of the histone code. Additionally, binding of *NEAT2* to unmethylated Pc2 promotes E2F1 SUMOylation, leading to activation of the growth-control gene program. These observations delineate a molecular pathway linking the actions of subnuclear structure-specific ncRNAs and nonhistone protein methylation to relocation of transcription units in the three-dimensional space of the nucleus, thus achieving coordinated gene expression programs.

INTRODUCTION

Regulated programs of gene expression are defined by the concerted interplay of transcriptional factors as well as other modulators such as epigenomic and signaling mediators. Recent studies have begun to elucidate the mechanistic control of gene expression by modulation of nuclear architecture and noncoding RNA (ncRNA) (Mercer et al., 2009; Misteli, 2010; Wilusz et al., 2009), suggesting the crosstalk between subnuclear architectural features and ncRNA as a possible mechanism for controlling gene expression. Thus, a growing number and type of molecular strategies combinatorially contribute to the precise control of gene expression involved in proliferation, differentiation, and maturation of cells.

In regulation of cell proliferation, the E2F family of transcription factors plays a critical role in organizing early cell-cycle progression by coordinating early cell-cycle events with the transcription of genes required for entry into S phase (Nevins, 1992). The transcriptional activity of E2F1 is regulated principally by association with different factors including the Rb–E2F complexes, which predominate in quiescent cells, acting as repressors of transcription (Bagchi et al., 1991). Other levels of control that influence E2F1 activity include its posttranslational modifications, protein stabilization (Campanero and Flemington, 1997), and regulation of its intracellular location (de la Luna et al., 1996).

At the level of "epigenomic control," a large and growing class of proteins, known as chromatin modifiers, constrains expression by adapting regions of the genome to maintain either gene silencing or gene activation (Kouzarides, 2007). Histone methylation, together with other site-specific modifications, plays an important role in the generation of specific molecular marks in chromatin, which are recognized by regulatory proteins, thus determining dynamic transitions between transcriptionally active and inactive states (Jenuwein and Allis, 2001). Recent data also show that the regulatory role of lysine methylation on proteins is not restricted to the "histone code" with this modification modulating activation, stabilization, and degradation of nonhistone proteins, thus influencing numerous cell processes (Huang and Berger, 2008). A number of histone methyltransferases (HMTases) that can methylate specific lysine residues of histones and certain nonhistone substrates have been identified and characterized (Chuikov et al., 2004; Sampath et al., 2007; Subramanian et al., 2008). Suv39h1 is an H3 lysine 9 methyltransferase containing the conserved SET domain and post-SET domains (Aagaard et al., 1999). It is documented that Suv39h1-mediated histone methylation functions in transcription

repression and gene silencing by recruitment of Polycomb proteins and forming and spreading heterochromatin (Lachner et al., 2001).

Genetic study of Suv39h1 transgenic mice has demonstrated that overexpression of Suv39h1 accelerates homeostatic cell proliferation (Czvitkovich et al., 2001), whereas Suv39h1/h2 double null mice have reduced viability during embryonic development and reduced growth as adult animals (Peters et al., 2001). Furthermore, Suv39h1 forms a complex with pRb/E2F1 and plays a role in the dynamic regulation of specific cell-cycle genes needed for entry into the S phase (Ait-Si-Ali et al., 2004; Nielsen et al., 2001). These observations suggest that Suv39h1 may function as a transcriptional corepressor of the E2F1 transcription factor. Indeed, Suv39h1 selectively interacts with vertebrate chromobox family (Cbx) proteins, including heterochromatin protein 1 (HP1) and Cbx4 (Pc2) (Sewalt et al., 2002). Although Cbx proteins are thought to function as repressors in heterochromatin formation and gene silencing, recent evidence has demonstrated that Cbx proteins also play a critical role in cell-cycle progression (Satijn et al., 1997). However, the role of Pc2 in cell-cycle regulation remains largely unknown.

The notion that ncRNAs can have numerous molecular functions is rapidly evolving (Eddy, 2001; Ponting et al., 2009). Even though long ncRNAs represent a large class of transcriptional units and appear to be evolutionarily conserved, their specific roles in critically modulating regulated gene expression remain poorly understood.

Here, we report a critical role of Suv39h1-mediated Pc2 methylation in regulating the cellular proliferation program, causing a relocation of growth-control gene loci from Polycomb bodies (PcGs) to interchromatin granules (ICGs) upon serum stimulation. We show that ncRNAs *TUG1* and *NEAT2* cause the growth-control genes to relocate from the repressive environment of PcG bodies, where they interact with corepressor complexes, to the gene activation milieu of the ICGs, by selectively interacting with methylated and unmethylated Pc2 present on growth-control gene promoters, respectively. Interaction with *NEAT2* regulates Pc2-dependent E2F1 SUMOylation, which licenses the recruitment of an H2B monoubiquitinase, CDCA7L, and biochemically switches the Pc2 chromodomain from preferring repressive histone marks to interacting with activation-associated histone marks. Broadly, our data highlight combinational actions of transcription factor/coregulators, nonhistone protein methylation, and ncRNAs resident in distinct subnuclear architectural structures as a central strategy to achieve coordinated programs of regulated gene expression, with implications for our understanding of the epigenomic programming in homeostasis and disease.

RESULTS

Pc2 Is a Substrate for Suv39h1, a Lysine-Specific Methyltransferase

We searched for nonhistone candidate substrates for Suv39h1 and found that Suv39h1 methylated Pc2 in vitro (Figures 1A and S1A–S1C). Under our assay conditions, Suv39h1-mediated methylation of Pc2 appeared to be quite specific. Other proteins such as SUMO1, SUMO-activating enzyme E1, E2, and E2F1 did not serve as Suv39h1 substrates (Figure 1A). Moreover, a Suv39h1 hyperactive mutant (H320R) (Rea et al., 2000) further enhanced the methylation of Pc2, whereas an enzymatically inactive Suv39h1 mutant (H324L) (Rea et al., 2000) failed to use Pc2 as substrate (Figures 1B and S1A). Trypsin digestion of immunoprecipitated FLAG-Pc2 from 293T cells coexpressed with wild-type (WT) Suv39h1 (Figure 1C, arrow), followed by mass spectrometry (MS), revealed that lysine 191 of Pc2 was dimethylated, which was not observed in cells overexpressed with enzymatically inactive Suv39h1 mutant (H324L) (Figure 1C and data not shown). A single K191R point mutation completely abolished Pc2 methylation, suggesting that K191 serves as a sole methylation site targeted by Suv39h1 (Figures 1D and S1D).

To investigate the role of Pc2 methylation in vivo, we generated rabbit polyclonal antibodies that specifically recognized dimethylated Pc2K191 and unmethylated Pc2 (Figure S1E). The anti-Pc2K191-dimethyl antibody (referred to as Pc2K191me^2 antibody) specifically detected bacterially purified Pc2 protein methylated by Suv39h1 in vitro but was totally unreactive against unmethylated Pc2 protein, whereas anti-Pc2K191 antibody (referred to as Pc2K191 antibody) specifically recognized unmethylated Pc2 protein with no cross-reaction to methylated Pc2 protein when equivalent amounts of methylated and unmethylated Pc2 were used (Figure 1E). We concluded that the Pc2K191me^2 and Pc2K191 antibodies specifically recognized K191-methylated and -unmethylated Pc2, respectively. To address whether Pc2 is methylated by Suv39h1 in vivo, we knocked down *Suv39h1* and other histone H3K9 methyltransferases including *Suv39h2*, *G9a*, *EuHMT*, and *ESET* by specific siRNAs in HeLa cells and observed that the Pc2K191me^2 level was specifically reduced only by *Suv39h1* siRNA compared to control siRNA, with a concurrent increase of unmethylated Pc2 level (Figures 1F and S1F). To rule out any potential off-target effects of *Suv39h1* siRNA, WT Suv39h1 or its enzymatically inactive mutant form (H324L) was transiently expressed in HeLa cells. Immunoblotting analysis using Pc2K191me^2 antibody detected increased levels of Pc2 methylation in extracts derived from cells overexpressing the WT Suv39h1, whereas cells equivalently transfected with the enzymatically inactive H324L mutant displayed minimal, if any, Pc2 methylation (Figure 1G). The expression levels of Suv39h1 proteins and the amount of total proteins in extracts were similar (Figure 1G). We therefore conclude that Suv39h1 methylates Pc2 at K191 in vivo.

Growth-Control Gene Activation Requires KDM4C-Mediated Pc2K191me^2 Demethylation

Interestingly, Pc2K191 exists in a sequence context resembling that of histone H3K9, which led us to search for candidate H3K9 demethylases that may demethylate Pc2K191me^2. By performing an in vitro demethylation assay using active FLAG-H3K9 demethylases purified from 293T cells (Figures S2A and S2B), we found that, in addition to histone H3K9me^2, KDM4C demethylated the dimethyl Pc2K191 (Figure 2A). Under our assay conditions, KDM4C-mediated demethylation of Pc2K191me^2 appeared to be quite specific, as other demethylases, including KDM3A, KDM4A, KDM4B, KDM4C, KDM4D, and PHF8, did not serve as Pc2K191me^2 demethylases although each of the purified demethylases exhibited robust enzymatic activity on an

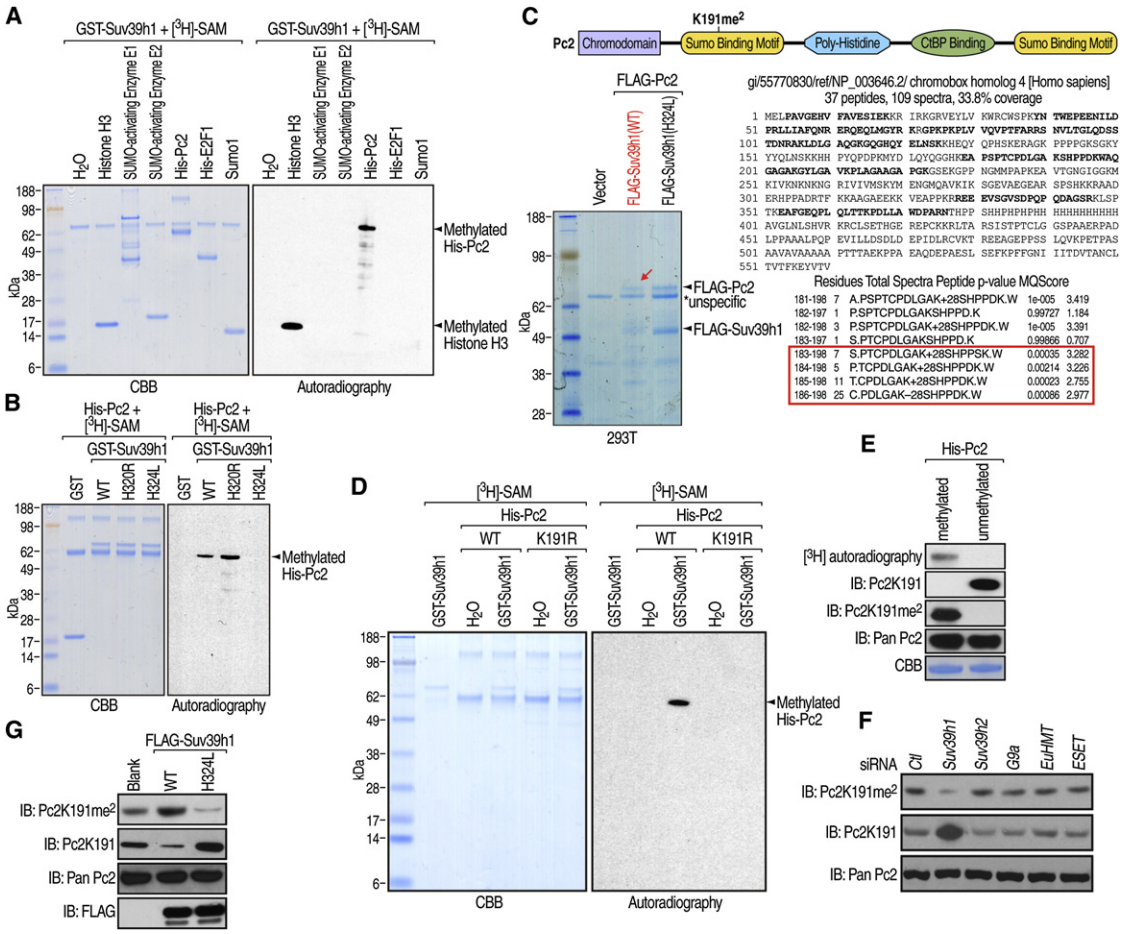

Figure 1. Suv39h1 Methylates Pc2 at K191

(A) Pc2 is a nonhistone substrate for Suv39h1. In vitro methylation assay was performed by incubating GST-Suv39h1 with recombinant His-Pc2, His-E2F1, histone H3, E1, E2, and SUMO1 in the presence of [^{3}H]-SAM.

(B) The enzymatic activity of Suv39h1 is required for Pc2 methylation. In vitro methylation assay was performed by incubating GST-Suv39h1 (WT, H320R, or H324L mutant) with His-Pc2 in the presence of [^{3}H]-SAM.

(C) Suv39h1 methylates Pc2 at K191 in vivo. FLAG-Pc2 immunoprecipitated from 293T cells (indicated by red arrow in left panel) was subjected to MOLDI-TOF analysis (right panel), and modified peptides are indicated by the red box.

(D) Suv39h1 methylates Pc2 at K191 in vitro. In vitro methylation assay was performed by incubating GST-Suv39h1 with WT Pc2 or K191R mutant in the presence of [^{3}H]-SAM.

(E) Validation of Pc2K191me^2 and Pc2K191 antibodies. Methylated and unmethylated His-Pc2 was subjected to autoradiography (top panel) or immunoblotting with antibodies indicated (middle panels).

(F and G) Suv39h1 methylates Pc2 at K191 in vivo. Cell lysates from HeLa cells transfected with siRNAs (F) or expression vectors (G) as indicated were immunoblotted with antibodies indicated.

For (A), (B), and (D), the reaction products were separated by SDS-PAGE followed by Coomassie blue staining (CBB) (left panel) or autoradiography (right panel). See also Figure S1.

H3K9me^2 substrate (Figure S2B). Moreover, the enzymatically inactive KDM4C-H190G/E192A mutant (Cloos et al., 2006) failed to demethylate Pc2K191me^2 (Figures 2B and S2C).

To investigate the potential role of Pc2 in cell-cycle and growth control, we next analyzed whether KDM4C-mediated demethylation of Pc2 regulates the transcriptional activation of E2F1 target genes. First, we examined whether Pc2K191me^2 level is physiologically regulated under the conditions of E2F1 activation. Immunoprecipitation experiments with Pc2K191me^2 and Pc2K191 antibodies revealed that Pc2K191me^2 levels exhibited a strong decrease in response to serum stimulation, concurrent with increased levels of unmethylated Pc2 (Figure 2C). We further examined the methylation status of Pc2 on E2F1 target gene promoters previously identified by E2F1 ChIP-seq (Liu et al., 2010), finding that Pc2K191me^2 specifically enriched on E2F1 target gene promoters, in contrast to no significant occupancy on the *Actin* promoter, which is not regulated by Polycomb proteins (Figure 2D, left panel). Importantly, Pc2K191me^2 levels dramatically decreased upon serum stimulation, which correlates with the increased levels of unmethylated Pc2 (Figure 2D,

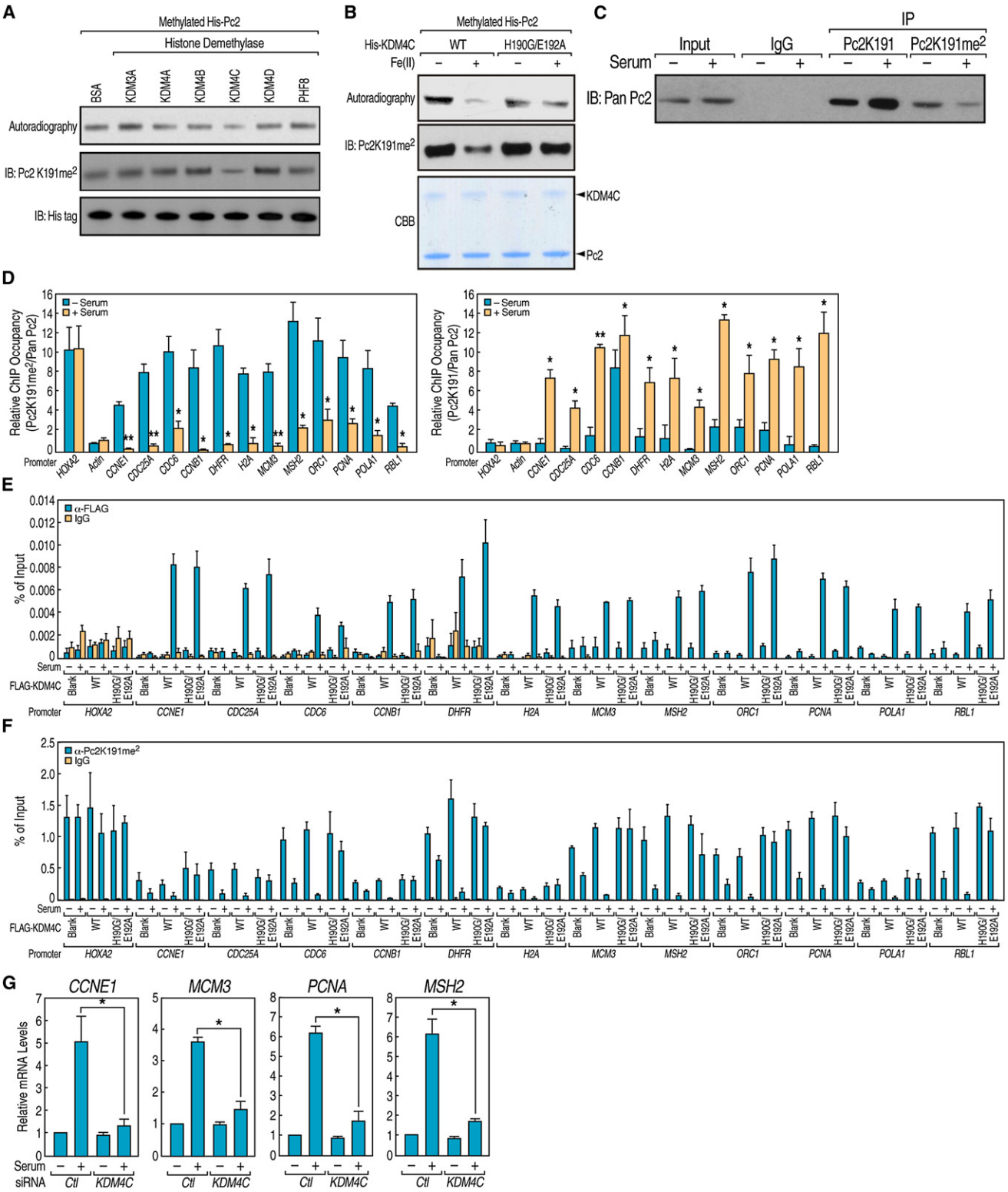

Figure 2. Growth-Control Gene Activation Requires KDM4C-Mediated Pc2K191me^2 Demethylation

(A) KDM4C demethylates Pc2 in vitro. Histone demethylase assay was performed by incubating purified FLAG-histone demethylases with in vitro methylated His-Pc2. Changes in substrate methylation levels were analyzed by autoradiography (upper panel) and Pc2K191me^2 antibodies (middle panel). Immunoblotting with antibodies against His tag was used to demonstrate equal loading (bottom panel).

right panel). Under the same conditions, the *HoxA2* promoter, on which Pc2 was consistently enriched, did not exhibit Pc2K191me^2 demethylation (Figure 2D).

Chromatin immunoprecipitation (ChIP) assays in HeLa cells transfected with KDM4C WT or H190G/E192A mutant revealed that serum stimulation resulted in increased recruitment of WT KDM4C on E2F1 target gene promoters (Figure 2E), which correlated with a decreased Pc2K191me^2 level (Figure 2F). The KDM4C-H190G/E192A mutant largely inhibited Pc2K191me^2 demethylation, despite being equally recruited on the same set of promoters (Figures 2E and 2F). Indeed, siRNA-mediated reduction of the levels of KDM4C also impaired the expression of E2F1 target genes upon serum stimulation in HeLa cells (Figures 2G and S2D). To further evaluate the alternative possibility that the actions of KDM4C that critically dictate growth-control gene expression might reside in its histone H3K9 demethylase activity, rather than actions on Pc2K191me^2, we took advantage of the previous observations that different H3K9 demethylases are utilized in a promoter-specific fashion to provide H3K9 demethylase activity (Fodor et al., 2006; Qi et al., 2010; Yamane et al., 2006). We found that growth-control gene promoters did not exhibit a KDM4C dependence on H3K9me^2 demethylation (Figure S2E, bottom panel), yet demethylase activity of KDM4C was required for the demethylation of Pc2K191me^2 and for activation for these growth-control genes (Figures S2E, top panel and 2G). Taken together, these data argue strongly that it is the specific demethylation of the repressive dimethyl Pc2K191 mark, caused by recruitment of KDM4C, rather than H3K9 demethylation, that is required for the transcriptional activation of E2F1 target genes.

Pc2 Methylation/Demethylation Controls the Cell-Growth Program

Considering the involvement of KDM4C-mediated Pc2K191me^2 demethylation on E2F1 target gene promoters in response to serum, we tested the possibility that Pc2 methylation/demethylation is required for controlling the growth-control gene expression and cell proliferation. Knockdown of *Pc2* in HeLa cells dramatically decreased serum-induced growth-control gene expression and cell proliferation (Figures 3A, 3B, and S3A). In accord with this finding, exogenous expression of Pc2 K191R mutant noticeably increased cell proliferation even at the basal level, further indicating that Pc2 is a potent regulator of the cell-growth program (Figure 3C).

The potential requirement of Pc2 in mitogenic signal-induced proliferation was next investigated in primary human fibroblasts. IMR-90 primary human lung fibroblasts became growth arrested with serum starvation and proliferated once released into serum-containing medium (Nahle et al., 2002). Immunoblotting showed that, although global Pc2 protein levels were not affected, serum stimulation of IMR-90 cells was largely accompanied by Pc2K191me^2 demethylation (Figure 3D). *Pc2* shRNAs (shPc2-1 and -2) dramatically reduced Pc2 protein levels when stably transduced into IMR-90 cells and impaired serum-induced cell proliferation (Figures 3E and S3B). Collectively, our data suggest that methylated Pc2 may represent an important antimitogenic signal and, under certain stimuli, a stress-induced modification mark required for growth-control gene repression and cell-cycle arrest, whereas unmethylated Pc2 is essential for physiological growth-control gene expression and cell proliferation.

Serum Induction Causes Relocation of E2F1-Regulated Genes between PcG Bodies and ICGs

We speculated that, given the involvement of Pc2 in stable gene repression (Lund and van Lohuizen, 2004), E2F1-regulated growth-control genes might relocate within the cell nuclei from transcriptional repressive PcG bodies to a transcriptionally permissive environment upon serum stimulation. We first examined the subnuclear localization of methylated and unmethylated Pc2. We observed that methylated Pc2 was concentrated in several defined domains that were faithfully costained with Bmi1 and Ring1A (Figures 4A and 4B), two well-established PcG body markers (Hernández-Muñoz et al., 2005). In contrast, unmethylated Pc2 showed strong colocalization only with SC35, a marker for the ICGs (Fu and Maniatis, 1990) (Figure 4C). Under our immunostaining conditions, colocalization of unmethylated Pc2 with ICGs appeared to be quite specific. Other nuclear bodies, including nuclear stress bodies, paraspeckles, Cajal bodies, and promyelocytic leukemia (PML) bodies, failed to exhibit costaining with unmethylated Pc2 (data not shown). We then performed immuno-FISH to test whether Pc2-associated E2F1 target transcription units relocated from PcG bodies to ICGs upon serum stimulation. Interestingly, gene loci encoding growth-control genes (*RBL1*, *MCM3*, *PCNA*, and *MSH2*) were found to predominantly colocalize with PcG bodies, as marked by Pc2K191me^2 staining (or Ring1A, see below) in serum-starved HeLa cells, and these loci largely colocalized with SC35-staining ICGs in the presence of serum (Figures 4D and S4A–S4C). Under

(B) Enzymatic activity of KDM4C is required for Pc2K191me^2 demethylation. His-KDM4C WT or H190G/E192A mutant was incubated with in vitro methylated His-Pc2 in the presence or absence of Fe (II). The reactions were separated by SDS-PAGE followed by autoradiography (upper panel), immunoblotting with Pc2K191me^2 antibodies (middle panel), or Coomassie blue staining (lower panel).

(C) Serum-induced demethylation of Pc2K191me^2 in vivo. HeLa cells were serum-starved followed by restimulation, and cell lysates were immunoprecipitated with Pc2K191 or Pc2K191me^2 antibodies followed by immunoblotting with pan Pc2 antibodies.

(D) Serum-induced demethylation of Pc2 on growth-control gene promoters. HeLa cells were serum-starved followed by restimulation, and ChIP analyses were performed using Pc2K191, Pc2K191me^2, and pan Pc2 antibodies on indicated regions. For each primer pair, Pc2K191me^2 (left panel) and Pc2K191 ChIP values (right panel) were normalized to the corresponding total pan Pc2 ChIP values.

(E and F) Serum-induced KDM4C recruitment is responsible for Pc2K191me^2 demethylation on growth-control gene promoters. HeLa cells transfected with blank vector, FLAG-KDM4C WT, or H190G/E192A mutant were serum-starved followed by restimulation, and ChIP analyses using FLAG antibody (E) or Pc2K191me^2 antibody (F) were performed on indicated regions.

(G) KDM4C is required for serum-induced growth-control gene expression. HeLa cells transfected with control or validated *KDM4C* siRNAs were serum-starved followed by restimulation, and relative mRNA levels of indicated genes were determined by qRT-PCR.

Mean ± SEM, *$p < 0.05$. See also Figure S2.

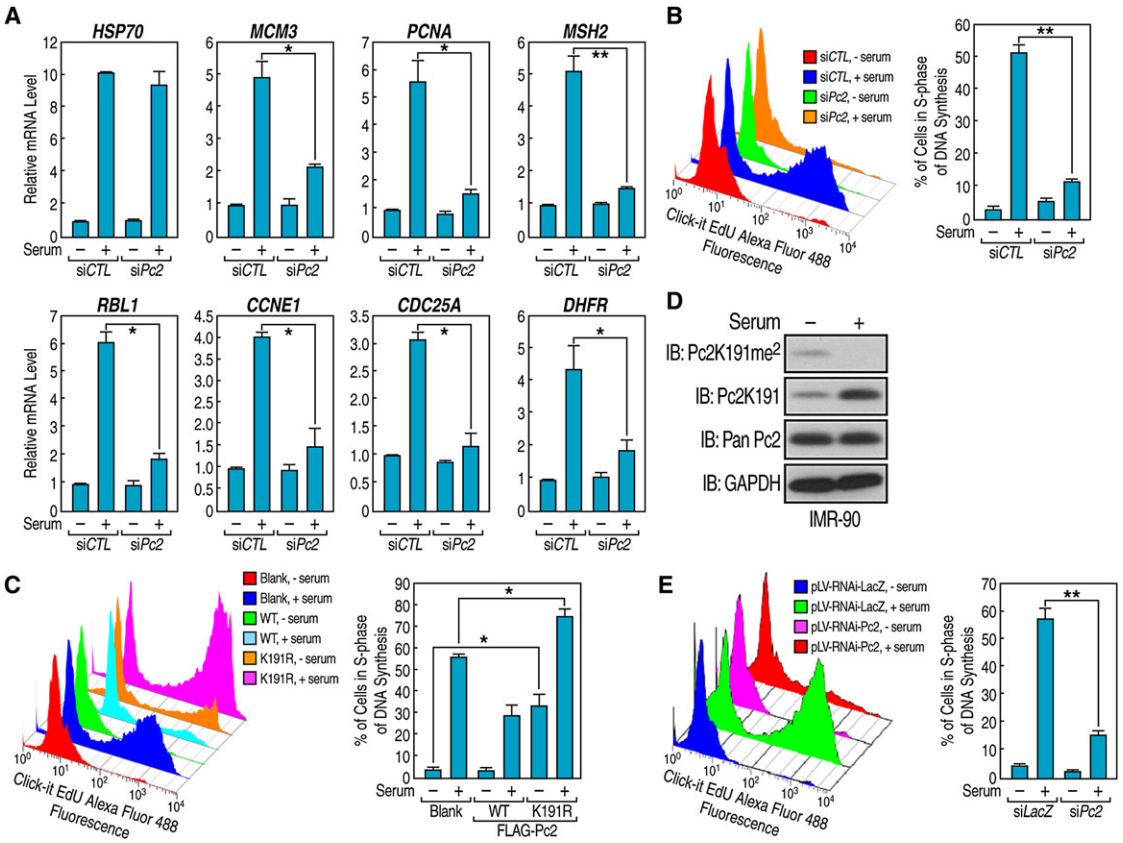

Figure 3. Pc2 Methylation/Demethylation Controls Mitogenic Signal-Induced Cell Proliferation

(A and B) Pc2 is essential for serum-induced growth-control gene expression and cell proliferation. HeLa cells transfected with *Pc2* siRNAs were serum-starved followed by restimulation, and mRNA levels of indicated genes (A) and cell proliferation (B) were analyzed, respectively.

(C) Pc2K191 methylation is a key regulator for cell proliferation. HeLa cells transfected with Pc2 plasmids (WT or K191R mutant) were serum-starved followed by restimulation, and cell proliferation was analyzed.

(D and E) IMR-90 cells were serum-starved followed by restimulation, and Pc2K191 methylation level (D) and cell proliferation (E) were analyzed by immunoblotting and flow cytometry, respectively.

For (B), (C), and (E), cell proliferation was analyzed by monitoring the EDU incorporation into DNA synthesis in S phase cells. Mean ± SEM, *$p < 0.05$ and **$p < 0.01$. See also Figure S3.

the same conditions, colocalization of E2F1 target gene loci with PcG bodies was reproducibly observed in immuno-FISH experiments using Ring1A, instead of Pc2K191me^2, staining as a marker for PcG bodies (Figure 4E). In contrast, unmethylated Pc2 specifically colocalized with activated E2F1 target gene loci upon serum stimulation (Figures S4D–S4G). It was previously shown that ICGs occupy the large space in nuclei, which results in a 14%–26% "unspecific" colocalization with genes under basal conditions (Szczerbal and Bridger, 2010). It is to be expected that any given gene locus may also exhibit a similar ~15%–25% "unspecific" colocalization with ICGs. To further support this assumption, we performed immuno-FISH on a cell-cycle-unrelated gene locus *BCR*, finding an average of ~10% and 30% colocalization of this locus with PcG bodies and ICGs in serum-starved cells, respectively, and that these colocalization percentages did not change upon serum stimulation (Figure S4H). Thus, given the assay background, the actual percent of relocation of growth-control genes from PcG bodies to ICGs would be considerably greater if this background were to be subtracted.

As expected, knockdown of *Pc2* impaired the colocalization of *MCM3* with both PcG bodies and ICGs (Figure 4F). Interestingly, other core components of the PRC1 complex including Bmi1 and PHC1 (Simon and Kingston, 2009) specifically interacted with methylated Pc2 (Figure 4G), and siRNA knockdown of these components disrupted the colocalization of *MCM3* with PcG bodies, but not ICGs, although having no obvious effects on maintenance of PcG bodies (Figures 4F, S4I, and S4J), suggesting that other components of the PRC1 complex may facilitate the repression of growth-control genes mediated by methylated Pc2 in PcG bodies.

We next tested whether demethylation of Pc2K191me^2 is required for the relocation process in HeLa cells microinjected with specific siRNAs against *KDM4C*, and we found that depletion of KDM4C largely abrogated dissociation of the *MCM3* gene locus from PcG bodies in the presence of serum stimulation (Figure 4H). In contrast, microinjection of plasmid encoding the Pc2K191R mutant in serum-starved cells resulted in dissociation of the *MCM3* gene locus from the Ring1A-stained PcG bodies,

while enhancing their colocalization with SC35-positive ICGs at basal level (Figure 4I). Together, these findings reveal an unexpected role of Pc2 in transcriptional regulation of growth-control genes by promoting the relocation of these gene loci from the transcriptionally repressive nuclear environment of PcG bodies to the transcriptionally permissive environment of ICGs. Given the observation that siRNA knockdown of *KDM4C* exerted no effect on serum-induced demethylation of H3K9me^2 on growth-control gene promoters (Figure S2E), we concluded that the KDM4C-dependent demethylation of Pc2K191me^2, rather than histones, appears to serve as the key determinant of the relocation of growth-control genes in response to growth signals.

Methylation Modulates Pc2 Association with ncRNAs

It has been reported that ncRNA may serve as a component to form subnuclear bodies and maintain their integrity (Bond and Fox, 2009). Given that methylated and unmethylated Pc2 are localized to PcGs and ICGs, respectively, and previous observations that the chromodomain is capable of binding RNA (Akhtar et al., 2000), we therefore tested the possibility that Pc2 might bind specific ncRNAs in these subnuclear structures. By performing in vivo *c*ross*l*inking and *i*mmuno*p*recipitation procedures (CLIP) using either Pc2K191me^2 or Pc2K191 antibodies, we observed that specific RNA-methylated Pc2 and RNA-unmethylated Pc2 complexes were formed after the UV crosslinking, which was significantly disrupted upon adding the blocking peptides for Pc2K191me^2 and Pc2K191 antibodies in cell lysates (Figure 5A). Sequence analysis of 94 different clones identified *TUG1*, a ncRNA interacting with EZH2 previously identified by RIP assay (Khalil et al., 2009) and repressing cell-cycle genes, as the most enriched RNA that interacted with methylated Pc2 (Figure S5A). Surprisingly, in the absence of K191 methylation, the predominant RNA associated with Pc2 was *NEAT2*/*MALAT1* (Figure S5B), an exclusive signature ncRNA for ICGs (Hutchinson et al., 2007). Likewise, purified biotinylated *TUG1* RNA (nt 117–3390) harboring the binding sequence identified in the CLIP assay specifically selected methylated Pc2 from HeLa cell nuclear extract, whereas biotinylated *NEAT2* RNA (nt 2281–5611) specifically bound unmethylated Pc2 (Figures 5B, S5C, and S5D). Electrophoretic mobility shift assays (EMSAs) were next used to analyze whether a direct switch of Pc2 RNA-binding preference is observed in response to K191 methylation. Incubation of the *TUG1* RNA probe with methylated Pc2 resulted in specific gel retardation (Figure 5C, first panel, lane 3), whereas incubation of only a 49 nt *NEAT2* RNA probe with unmethylated Pc2 specifically resulted in gel shift (Figure 5C, third panel, lane 4). Under these conditions, no shift was observed when the corresponding *TUG1* and *NEAT2* DNA probes or cold probes were used (Figures 5C and S5E). We, therefore, conclude that the interactions of methylated or unmethylated Pc2 with ncRNAs are controlled by a specific covalent modification of Pc2.

ncRNA-Pc2 Interactions Underlie Relocation and Transcriptional Regulation of Growth-Control Genes

Pc2 has been characterized as a "reader" for the histone code through its chromodomain (Bernstein et al., 2006). To gain insight into whether binding of ncRNAs affects the histone code reading ability of Pc2, we carried out a modified histone peptide array analysis in an open-ended manner. Consistent with a previous publication (Bernstein et al., 2006), bacterially purified chromodomain of Pc2 specifically recognized histone H3K9me^3 (Figures 5D and S5F). Strikingly, in the presence of *TUG1* ncRNA, the Pc2 chromodomain now instead read both H4R3me^{2s} and H3K27me^2 (Figures 5E and S5G), which are associated with global gene repression (Xu et al., 2010). In contrast, by binding to *NEAT2* RNA, Pc2 switched from an H3K9me^3 reader to preferentially binding H2AK5ac and H2AK13ac, marks of gene activation (Figures 5F and S5H). As controls, *TUG1* (117–3390) or *NEAT2* (2281–5611) alone failed to bind any histone marks (Figures S5I and S5J). Collectively, our results now suggest a mechanism by which ncRNAs can regulate reading of the histone code by chromatin-binding domains of various regulatory cofactors. In this case, ncRNA interacting with a chromodomain switches preferential binding from repressive to activation histone marks.

ICG-specific localization of *NEAT2* (Hutchinson et al., 2007) led us to examine the cellular localization of *TUG1* by utilizing a molecular beacon targeting *TUG1*. Single-cell nuclear microinjection of the *TUG1* molecular beacon followed by immunostaining suggested that part of *TUG1* localization overlapped with methylated Pc2 staining, suggesting the localization of *TUG1* within the PcG bodies (Figure 5G). Thus, the subnuclear structure-specific localization of *TUG1* and *NEAT2* may indicate that they serve as the actual docking sites responsible for relocation of Pc2-bound growth-control gene promoters. Indeed, knockdown of *TUG1* caused a dramatic redistribution of growth-control gene promoters out of PcG bodies (Figures 5H and S5K), which correlated with increased gene expression (Figure 5I) and cell proliferation, even in the absence of serum (Figure 5J). Conversely, removal of *NEAT2* disrupted the colocalization of the *MCM3* gene locus with ICGs (Figures 5H and S5K) and caused loss of serum-induced gene expression (Figure 5I) and of cell proliferation (Figure 5J), although structures of the PcG bodies and ICGs were not discernibly affected by knocking down *TUG1* (Figure S5L) and *NEAT2* (Clemson et al., 2009) and serum treatment (Figure S5M).

Next, we used RNA pull-down experiments to identify the proteins associated with *TUG1* and *NEAT2*. The experiment performed here calls for washes with buffer containing 1000 mM salt, which definitively results in relatively low backgrounds in pull-downs and does not disrupt association of *TUG1* and *NEAT2* with proteins. MS analysis on proteins pulled down by biotinylated *TUG1* and *NEAT2* revealed that *TUG1* RNA specifically bound to a number of proteins involved in transcriptional repression, including histone methyltransferases/demethylases and chromatin modifiers (Figure 5K; Tables S1 and S2), whereas *NEAT2* RNA bound to functionally distinctive cofactors associated with gene activation including transcriptional coactivators, histone methyltransferases/demethylases associated with transcriptional activation, and pre-mRNA splicing factors (Figure 5K; Tables S1 and S3), suggesting that ncRNAs may impose a chromatin-remodeling environment by selectively interacting with chromatin modifier proteins. Intriguingly, *TUG1* interacted with Coronin2A, which is a corepressor based on actin oligomerization (Huang et al., 2011), whereas

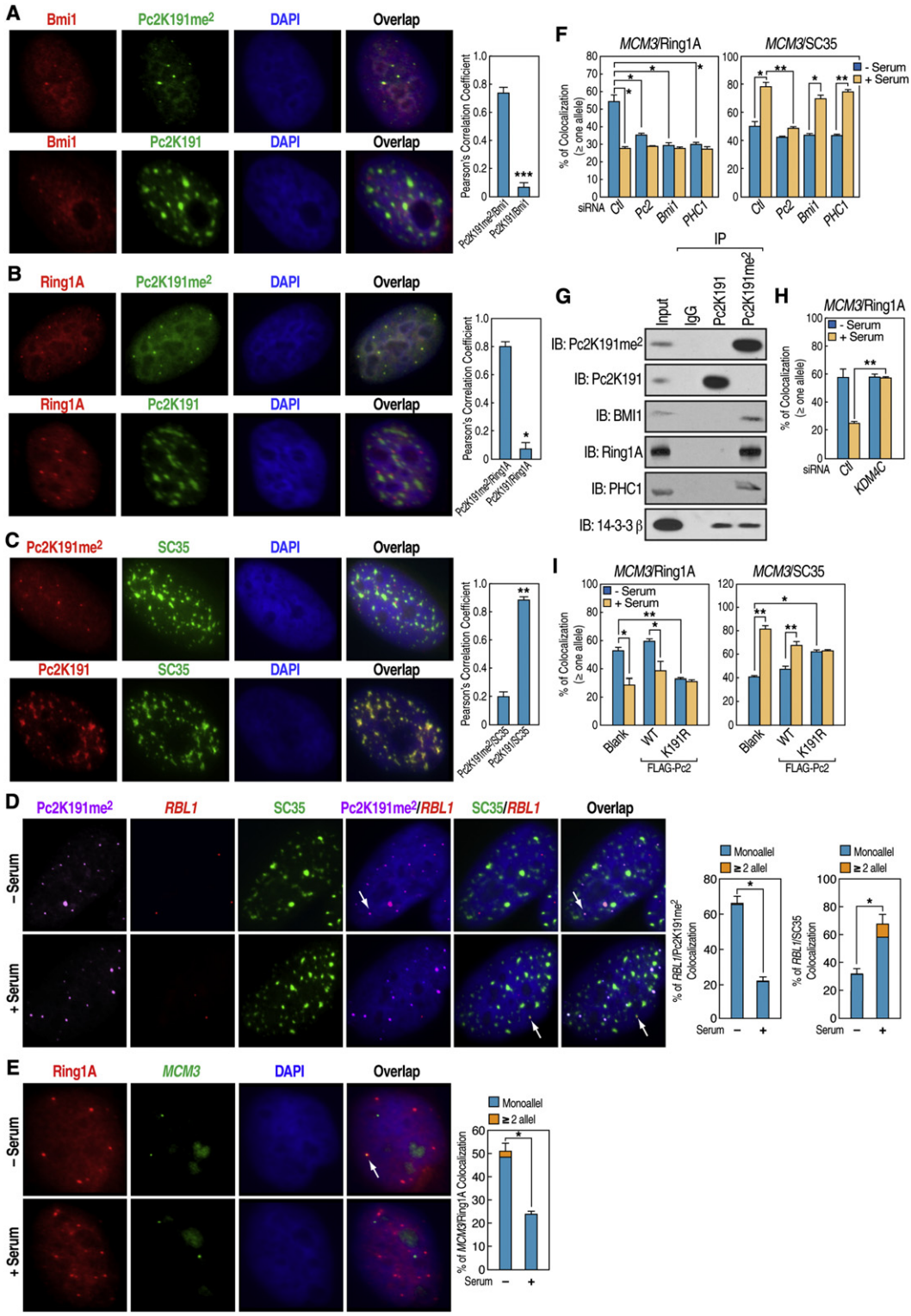

Figure 4. Relocation of E2F1-Regulated Growth-Control Genes from PcG Bodies to ICGs following Serum Induction

(A–C) Methylated and unmethylated Pc2 exhibit distinct immunostaining patterns with respect to Bmi1 (A) or Ring1A (B) as a marker of PcG bodies and SC35 (C) of ICGs.

(D and E) Serum-induced relocation of growth-control gene locus between PcG bodies and ICGs. HeLa cells were serum-starved followed by restimulation, and immuno-FISH analyses were performed using antibodies against Pc2K191me^2 (D) or Ring1A (E) and FISH probes targeting *RBL1* (D) or *MCM3* (E).

LSD1 interacted with *NEAT2*, consistent with previous observations that LSD1 colocalizes with transcription units in ICGs (Hu et al., 2008).

Unmethylated Pc2 Mediates Serum-Induced E2F1 SUMOylation

We next examined the functional roles of unmethylated Pc2 in growth-control gene activation. Immunoblotting of E2F1 immunoprecipitates from denatured cell lysates unexpectedly revealed an upshifted E2F1 band induced by serum stimulation, which was not due to an E2F1-associated protein but rather a posttranslational modification (Figures 6A and S6A). Immunoblotting using antibody specific against SUMO1 and SUMO2/3 confirmed that E2F1 and E2F6, but not E2F4, were SUMO1 modified (Figures 6A, S6B, and S6C). In searching for cellular components responsible for E2F1 SUMOylation, we observed a decreased E2F1 SUMOylation with depletion of Ubc9 and Pc2, but not other candidate E3 ligases tested (Figures 6B and S6D). When Pc2 was cotransfected with Myc-SUMO1, we observed a significant increase in E2F1 SUMOylation in vivo (Figure S6E). The fact that Pc2 directly mediated E2F1 SUMOylation was further confirmed in vitro (Figure 6C). To map the SUMOylation site, charge-conserving E2F1 lysine to arginine point mutants were tested for SUMOylation, revealing that the E2F1 K266R mutant showed deficient SUMOylation both in vivo and in vitro (Figures 6D, 6E, and S6F). Although E2F1 and E2F1 K266R localized equally on the promoters of E2F1 target genes, the E2F1 K266R mutant largely inhibited serum-induced gene expression, which was not due to any effects of K266R mutation on E2F1 stability or its interaction with Rb (Figures 6F, S6G, and S6H). Together, these results have revealed a requirement for Pc2-mediated E2F1 K266 SUMOylation or stabilization of this SUMOylation for the transcriptional activation of growth-control genes.

The observation that expression of the Pc2K191R mutant, which exerted no effects on endogenous levels of Ubc9, noticeably enhanced E2F1 SUMOylation (Figures 6G and S6I) led us to explore whether ncRNAs might modulate E2F1 SUMOylation mediated by Pc2. We first tested whether Pc2-regulated E2F1 SUMOylaton was RNA dependent. Treatment of Pc2K191me^2 immunoprecipitates with RNase I slightly enhanced E2F1 SUMOylation, whereas the same treatment impaired E2F1 SUMOylation mediated by Pc2K191 immunoprecipitates (Figure 6H). Consistently, the inhibitory activity of *TUG1* on E2F1 SUMOylation was observed in performing an in vitro SUMOylation assay, with the addition of *TUG1* RNA abolishing the enhanced E2F1 SUMOylation mediated by methylated Pc2 (Figure 6I, right panel, lane3). Taken together, our findings suggest that Pc2-mediated E2F1 SUMOylation at K266, which was modulated by interactions with ncRNAs, is required for the activation of cell-growth-control genes in response to serum.

CDCA7L Links E2F1 SUMOylation and H2B Ubiquitination in Growth-Control Gene Activation

The functional binding of SUMOylated proteins to the SUMO-interacting motif (SIM)-containing proteins plays critical roles in many biological processes including transcriptional activation, cell growth/differentiation, and DNA-damage response (Kerscher, 2007). Thus, we searched for the potential SIM-containing proteins that can recognize the E2F1 K266 SUMOylation and its functional role in regulating growth-control gene activation. Analysis by MS of a protein exclusively copurified with WT E2F1, but not the K266R mutant, identified it as CDCA7L/JPO2/RAM2 (Figures 7A, S7A, and S7B), a cell-cycle regulator with a conserved RING domain (Huang et al., 2005). The specific interaction between SUMOylated E2F1 and CDCA7L was mediated by a SIM located N-terminal of CDCA7L, and mutations in this motif (V100/103A) abolished the interaction with SUMOylated E2F1 (Figure 7B). Consistent with the specific recruitment of CDCA7L on the E2F1 target gene promoters upon serum stimulation (Figure 7C), knockdown of *CDCA7L* by shRNAs blocked serum-induced expression of E2F1 target genes (Figures 7D and S7C). CDCA7L possesses a conserved RING finger domain, a characteristic of RING-class E3 ubiquitin protein ligases (Deshaies and Joazeiro, 2009). We therefore screened potential substrates of CDCA7L by both in vivo and in vitro ubiquitination assay, finding that CDCA7L strongly stimulated H2B monoubiquitination at K120 (Figures S7D–S7F). These results indicate that the RING finger of CDCA7L is required for the monoubiquitination of H2B, and perhaps additional substrates, critical for transcriptional activation of growth-control genes.

Analysis by ChIP assay of UbH2B and H2B enrichment revealed that ubiquitination of H2B was enhanced at the E2F1-binding sites upon serum stimulation, which was diminished with knockdown of *CDCA7L* (Figure 7E). This finding is consistent with the previous notion that UbH2B correlates with gene activation and transcriptional elongation (Minsky et al., 2008). Together, these data revealed that a series of covalent modifications initiated by Pc2-mediated SUMOylation of E2F1 leads to the subsequent H2B ubiquitination and the activation of a cohort of growth-control genes.

(F) Effect of knockdown of *Pc2*, *Bmi1*, and *PHC1* on relocation of *MCM3* locus between PcG bodies and ICGs. HeLa cells microinjected with indicated siRNAs were serum-starved followed by restimulation, and immuno-FISH analyses were performed using antibodies and FISH probes as indicated.

(G) Interaction between endogenous Pc2 and other core components of the PRC1 complex demonstrated by coimmunoprecipitation of Pc2K191me^2 with Bmi1, Ring1A, and PHC1 in HeLa cell extracts. The input represents 10% of the protein amount used for immunoprecipitation.

(H) KDM4C is required for serum-induced dissociation of the *MCM3* locus from PcG bodies. HeLa cells microinjected with control siRNA or validated siRNA against *KDM4C* were serum-starved followed by restimulation, and immuno-FISH analyses were performed using Ring1A antibodies and probes targeting the *MCM3* locus.

(I) Demethylated Pc2 is required for relocation of the *MCM3* locus. HeLa cells microinjected with blank vector, Pc2 WT, or K191R mutant were serum-starved followed by restimulation, and immuno-FISH analyses were performed using Ring1A, SC35 antibodies, and probes targeting the *MCM3* locus. Statistical analyses on colocalization of *MCM3* locus with Ring1A staining (left panel) and SC35 staining (right panel) were shown.

For (A), (B), (C), (D), and (E), left panels show representative images, and right panels show statistical analyses. Mean ± SEM, *$p < 0.05$ and **$p < 0.01$.

See also Figure S4.

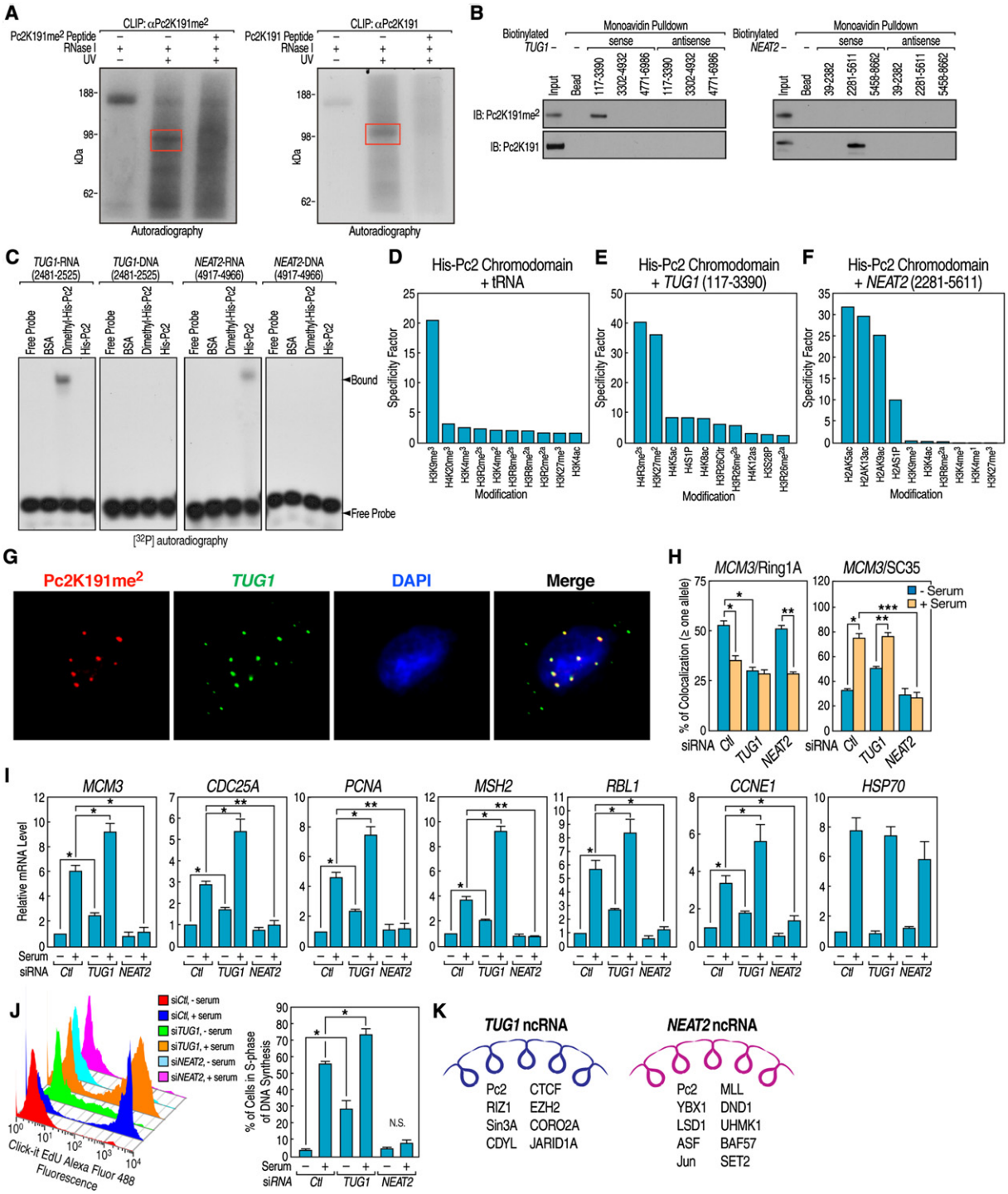

Figure 5. ncRNA-Pc2 Interactions Underlie Relocation and Transcriptional Activation of Growth-Control Genes

(A) Methylated and unmethylated Pc2 bind to RNAs. CLIP assays using Pc2K191me^2 (left panel) or Pc2K191 (right panel) antibodies were performed, and specific protein-RNA complexes (indicated by red box) were visualized by autoradiography.

(B) Validation of interactions of *TUG1* and *NEAT2* with Pc2. In vitro transcribed biotinylated *TUG1* RNA (left panel) or *NEAT2* RNA (right panel) were incubated with HeLa nuclear extract. The elution of Monoavadin beads was subjected to immunoblotting with indicated antibodies.

(C) The selective binding of Pc2 to *TUG1* or *NEAT2* depends on K191 methylation state. RNA gel shift assay was performed using synthesized *TUG1* and *NEAT2* RNA and their corresponding DNA oligos and recombinant His-Pc2 with or without in vitro methylation.

(D–F) *TUG1* and *NEAT2* function as modulators of Pc2 chromodomain for "reading" the histone code. modified histone peptide array was incubated with recombinant His-Pc2 chromodomain in the presence of yeast tRNA (D), in vitro transcribed *TUG1* (117–3390) (E), or *NEAT2* (2281–5611) (F) RNA fragments and

DISCUSSION

Orchestrating precise spatial and temporal patterns of gene expression is crucial for the normal development of all organisms and maintenance of homeostasis. DNA-binding transcription factors, chromatin modifiers, and dynamic positioning of particular loci in nuclei are all essential to establish precise transcriptional regulation and achieve the correct patterns of gene expression. Here, we have elucidated how a nonhistone methylation event and the resultant specific ncRNA associations spatially modulate signal-induced nuclear architecture alteration, which underlies regulation of transcription units controlling cell-growth programs in both normal and transformed cells.

Our studies have revealed that the methylation/demethylation of a single protein associated with E2F1-bound growth-control genes, Pc2, is responsible for the physical relocation of these transcription units from PcG bodies, in which their expression is repressed, to ICGs, in which their expression is activated (Figure 7F). Unexpectedly, this reflects the differential interactions of methylated versus unmethylated Pc2 with two distinct ncRNAs that are located in distinct subnuclear architectural compartments (Figure 7F). In the case of Pc2, methylation controls the protein's interaction with two distinct ncRNAs, *TUG1* and *NEAT2*, which results in the exclusive subnuclear localization of methylated and unmethylated Pc2 in PcG bodies and ICGs, respectively. Methylated Pc2 may represent an important antimitogenic signal and, under certain stimuli, a stress-induced modification mark required for growth-control gene repression and senescence, whereas unmethylated Pc2 is essential for physiological growth-control gene expression and cell proliferation.

TUG1, previously reported to interact with the PRC2 complex (Khalil et al., 2009), is localized in PcG bodies to serve as a scaffold by interacting with Suv39h1-methylated Pc2, which relocates growth-control transcription units and brings them in proximity with specific corepressor machinery. In contrast, *NEAT2* interacts with several proteins associated with gene activation. These ncRNAs promote the relocation of growth-control genes in response to mitogenic signals and are likely to facilitate the repression/activation of the encoded transcription units based both on their association with multiple coregulating complexes and on actions to modulate histone marks preferred by "readers" of the histone code. Indeed, the loss of *TUG1* causes signal-independent activation of growth by failure to recruit growth-control gene loci to PcG bodies, whereas, conversely, the loss of *NEAT2* inhibits growth, even in the presence of growth signals, with a failure to relocate the growth-control genes to ICGs.

This dynamic process is apparently dependent on a histone demethylase, KDM4C, that facilitates signal-dependent relocation of growth-control genes between distinct subnuclear architectural structures, with two ncRNAs serving as subnuclear molecular scaffolds. Our data have thus identified Pc2-ncRNA interactions as a key mechanism that determines the relative positioning of a growth-control gene regulatory program with respect to subnuclear architectural structures; however, we cannot absolutely exclude the possibility of a rapid assembly of subnuclear architectural structures in situ on the regulated promoters.

Consistent with our ncRNA pull-down results, the promoters interacting with *TUG1* are postulated to present multiple epigenomic regulators that might also modulate histone marks, including the H3K9 methyltransferase RIZ1, the H3K27 methyltransferase EZH2, and the H3K4 demethylase JARID1A. In contrast, the promoters associated with *NEAT2* in ICGs exhibit low levels of H3K9me$^{2/3}$ but high levels of H3K36me^{3} and H3K4me^{3}, perhaps regulated by interaction of *NEAT2* with LSD1, SET2, and MLL. These data suggest the potential importance of these two ncRNAs as platforms for organizing a coordinated repression or activation program, respectively.

Taken together, our findings highlight the large network of long ncRNAs, together with their associated protein complexes, as key components of the subnuclear architectural structures, each acting as a "sensor" for specific cohorts of regulated gene programs in response to signal-induced modifications that license gene-regulatory region-ncRNA interactions. Although Pc2 methylation appears to be the key determinant for relocation of growth-control genes, based on a methylation/demethylation-dependent switch in preference for *TUG1* or *NEAT2* interactions, respectively, we are tempted to speculate that other ncRNAs recognize covalent modifications of other gene-associated proteins and exert their ncRNA scaffold functions in distinct subnuclear compartments to act as sensors for many regulated signaling pathways, and as modulators of "reading" marks on histone tails for a variety of chromodomain-containing proteins and other histone code "readers."

Future exploration of interactions between subnuclear structure-specific ncRNAs and functionally distinctive protein cohorts is likely to uncover fresh insights into central strategies in development, homeostasis, and disease.

subjected to immunoblotting with indicated antibodies. The Myc tag antibody was added to detect Myc-tagged peptides on position P21 as positive control. The binding specificity calculated by Array Analyses Software based on two arrays (images shown in Figures S5F–S5H) was shown.

(G) *TUG1* is localized in PcG bodies. HeLa cells microinjected with molecular beacon probes targeting *TUG1* were subjected to immunostaining with Pc2K191me^{2} antibodies.

(H) *TUG1* and *NEAT2* are required for serum-induced relocation of the *MCM3* locus. HeLa cells microinjected with validated siRNA targeting *TUG1* or *NEAT2* were serum-starved followed by restimulation, and immuno-FISH analyses were performed using Ring1A, SC35 antibodies, and probes targeting the *MCM3* locus. Statistical analyses on colocalization of *MCM3* loci with Ring1A staining (left panel) and SC35 staining (right panel) are shown.

(I and J) Effect of *TUG1* or *NEAT2* knockdown on serum-induced growth-control gene expression and cell proliferation. HeLa cells transfected with *TUG1* or *NEAT2* siRNA were serum-starved followed by restimulation, and relative mRNA levels of indicated genes and cell proliferation were determined by qRT-PCR (I) and flow cytometry (J).

(K) A list of *TUG1* and *NEAT2* ncRNA-associated proteins identified from two independent MS experiments.

Mean ± SEM, *$p < 0.05$, **$p < 0.01$, and ***$p < 0.001$. See also Figure S5 and Tables S1, S2, and S3.

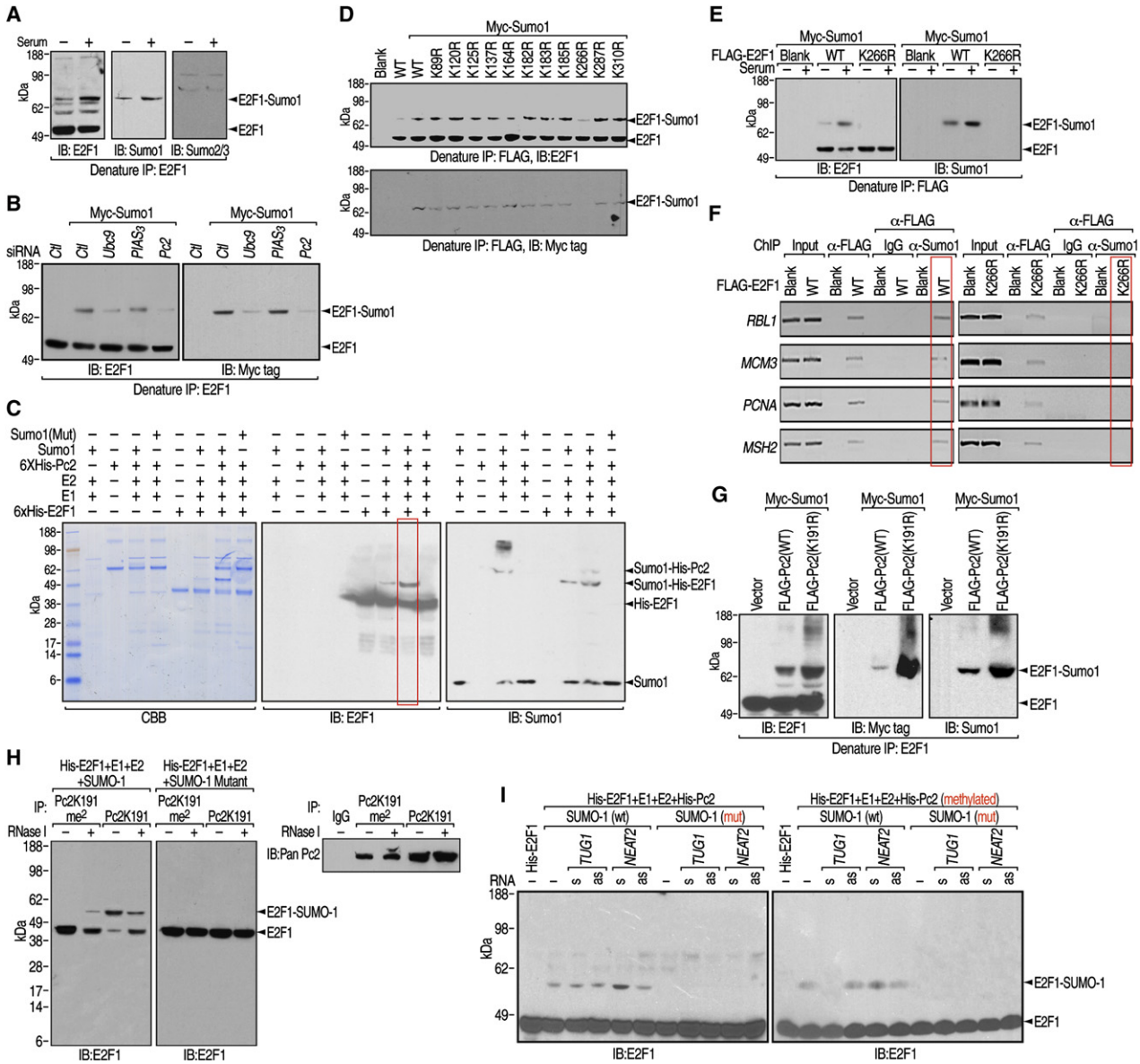

Figure 6. Pc2-Mediated E2F1 SUMOylation Is Required for Growth-Control Gene Activation

(A) Serum-induced E2F1 SUMOylation. HeLa cells were serum-starved followed by restimulation, and the cell lysates were immunoprecipitated with E2F1 antibodies under denaturing conditions followed by immunoblotting with antibodies indicated.

(B) Pc2 promotes E2F1 SUMOylation in vivo. HeLa cells were transfected with indicated siRNAs/plasmids, and the cell lysates were immunoprecipitated with E2F1 antibodies under denaturing conditions followed by immunoblotting with E2F1 (left panel) or Myc tag (right panel) antibodies.

(C) Pc2 promotes E2F1 SUMOylation in vitro. Bacterially expressed His-Pc2 and His-E2F1 were incubated with recombinant E1, E2, and SUMO1 or SUMO1 mutant. The reactions were separated by SDS-PAGE followed by Coomassie blue staining (left panel) and immunoblotting with E2F1 (middle panel) or SUMO1 (right panel) antibodies.

(D and E) E2F1 is SUMOylated at lysine 266. HeLa cells were transfected with WT or single K mutated E2F1 (D) or K266R mutant (E) as indicated, and the cell lysates were immunoprecipitated with FLAG antibodies under denaturing conditions followed by immunoblotting with E2F1 (upper panel) or Myc tag (bottom panel) antibodies (D) and E2F1 (left panel) or SUMO1 (right panel) antibodies (E).

(F) E2F1 SUMOylation on growth-control gene promoters. HeLa cells were transfected with indicated plasmids followed by two-step ChIP analyses using FLAG and SUMO1 antibodies on indicated regions.

(G) K191 methylation inhibits Pc2-mediated E2F1 SUMOylation in vivo. HeLa cells were transfected with indicated plasmids, and the cell lysates were immunoprecipitated with E2F1 antibodies under denaturing conditions followed by immunoblotting with E2F1 (left panel), Myc tag (middle panel), or SUMO1 (right panel) antibodies.

(H) Pc2-mediated E2F1 SUMOylation is RNA dependent. Immunoprecipitates of Pc2K191me^2 or Pc2K191 from HeLa cells (right panel) were incubated with His-tagged E2F1, recombinant E1, E2, and SUMO1 or SUMO1 mutant with or without RNase I treatment. The reaction products were subjected to immunoblotting using antibodies targeting E2F1 (left panel).

EXPERIMENTAL PROCEDURES

Cell Culture

Human cervical cancer cell line HeLa, embryonic kidney cell line HEK293T, and human lung normal fibroblast IMR-90 were obtained from American Type Culture Collection (ATCC) and were cultured under standard conditions. Transfection of HeLa cells with siRNA and plasmid DNA was performed using Lipofectamine 2000 (Invitrogen). To induce growth-control gene expression and cell proliferation, HeLa cells transfected with plasmids or siRNAs as indicated were starved in serum-free media for 48 hr followed by stimulation with complete serum media for an additional 16 hr. IMR-90 fibroblasts were incubated in DMEM (GIBCO) medium supplemented with a suboptimal concentration of FBS (0.1%) for 4 days. Normal serum level (10%) was restored, and cells were harvested at 24 hr after release from low serum. A detailed description of methods is included in the Extended Experimental Procedures.

Antibody Generation

The rabbit anti-dimethyl-Pc2-specific antibody (Pc2K191me^2) was raised against a synthetic peptide CPDLGA (dimethyl-K) SHPPDKWAQ based on the human Pc2 sequence flanking lysine 191 (Abgent). The rabbit anti-unmethylated Pc2 antibody (Pc2K191) was obtained at the same time against peptide CPDLGAKSHPPDKWAQ (Abgent). The Pc2K191me^2 and Pc2K191 antibodies were used for immunoprecipitation, immunoblotting, ChIP, CLIP, and immunofluorescence.

Cell Proliferation Assay

Cell proliferation was measured by using the Click-iT EdU Cell Proliferation Assay Kit (Invitrogen) following the manufacturer's protocol. Data were recorded on a BD LSR II Flow Cytometer and analyzed by FlowJo flow cytometry analysis software (Tree Star, Inc.).

Immunofluorescence and Colocalization Analyses

Immunofluorescence of HeLa cells was carried out as previously described (Liu et al., 2010). Images were acquired with a Zeiss Axioplan 2MOT Epifluorescent microscope (Carl Zeiss, Inc) and Hamamatsu ORCA ER black/white CCD camera in 63× oil immersion objective with each channel recorded once and all channels overlapped to generate overall images. For Ring1/Bmi1 and Pc2K191me^2 immunofluorescence, rabbit anti-Ring1/Bmi1 and anti-Pc2K191me^2 IgGs were labeled by Zenon Alexa Fluor 594 and 488 Rabbit IgG Labeling Kits, respectively (Molecular Probe).

Quantification of colocalization was determined by Pearson's correlation coefficient using commercially available Colocalizer Pro software, and the analysis was performed on at least 100 cells per condition with three independent experiments.

Immunofluorescence In Situ Hybridization

Cell nuclei isolation and immuno-FISH were carried out according to a method previously described (Lavrov et al., 2004), and the probes were commercially labeled by Empire Genomics and are listed in Extended Experimental Procedures. At least 100 cells were counted in each experiment for statistical analysis.

In Vivo Crosslinking and Immunoprecipitation Assay

CLIP analyses of methylated and unmethylated Pc2 were performed as previously described (Ule et al., 2005). Briefly, cells were ultraviolet (UV) irradiated to covalently crosslink RNA-protein complexes. After UV irradiation, cells were lysed, and the RNA was partially digested, allowing a small fragment to remain attached to protein. RNA-protein complexes of interest were then partially purified by immunoprecipitation, and noncovalently associated RNAs were removed by sodium dodecyl sulfate polyacrylamide gel electrophoresis (SDS-PAGE). These purified RNA-protein complexes were isolated and treated with proteinase K, which removes protein but leaves intact RNAs. The recovered RNAs were subjected to RNA linker ligation, RT-PCR amplification, and sequencing.

Molecular Beacon and RNA FISH

Custom-designed molecular beacon targeting *TUG1* was synthesized by IDT. RNA FISH was performed using Stellaris RNA FISH technology according to manufacturer's instruction (Biosearch Technologies, Inc.). Stellari RNA FISH probes targeting *TUG1* and *NEAT2* were designed at http://www.singlemoleculefish.com/designer.html.

Data Analysis and Statistics

Relative quantities of gene expression level were normalized to *Actin*. The relative quantities of ChIP samples were normalized by individual inputs, respectively. Results are reported as mean ± standard error of the mean (SEM) of three independent experiments. Comparisons were performed using two-tailed paired Student's t test. *$p < 0.05$, **$p < 0.01$, and ***$p < 0.001$.

SUPPLEMENTAL INFORMATION

Supplemental Information includes Extended Experimental Procedures, seven figures, and three tables and can be found with this article online at doi:10.1016/j.cell.2011.08.054.

ACKNOWLEDGMENTS

We thank C. Nelson for assistance with cell culture; J. Hightower for artwork; D. Benson, M. Fisher, and R. Pardee for assistance with the manuscript; Dr. B. Tanasa for providing E2F1 target sites from previously published ChIP-Seq data; Dr. P. Sun and Dr. R. Liao for providing BJ cells and technical support for the senescence study; Dr. R. June for assistance with flow cytometry analysis; and Dr. M. Ghassemian and Wei Ting Liu for mass spectrometry analysis. Michael G. Rosenfeld is a Howard Hughes Medical Institute Investigator. This study was funded by grants from DK018477, DK74868, DK39949, CA97134, NS34934, W81XWH-08-1-0665, and the Prostate Cancer Foundation to M.G.R.; L.Y. is the recipient of a DoD Era of Hope Postdoctoral Award (W81XWH-08-1-0554); and C.L. is the recipient of a Susan G. Komen for the Cure Fellowship (KG080247).

Received: November 10, 2010
Revised: May 5, 2011
Accepted: August 26, 2011
Published: November 10, 2011

REFERENCES

Aagaard, L., Laible, G., Selenko, P., Schmid, M., Dorn, R., Schotta, G., Kuhfittig, S., Wolf, A., Lebersorger, A., Singh, P.B., et al. (1999). Functional mammalian homologues of the Drosophila PEV-modifier Su(var)3-9 encode centromere-associated proteins which complex with the heterochromatin component M31. EMBO J. *18*, 1923–1938.

Ait-Si-Ali, S., Guasconi, V., Fritsch, L., Yahi, H., Sekhri, R., Naguibneva, I., Robin, P., Cabon, F., Polesskaya, A., and Harel-Bellan, A. (2004). A Suv39h-dependent mechanism for silencing S-phase genes in differentiating but not in cycling cells. EMBO J. *23*, 605–615.

Akhtar, A., Zink, D., and Becker, P.B. (2000). Chromodomains are protein-RNA interaction modules. Nature *407*, 405–409.

(I) *TUG1* and *NEAT2* regulate Pc2-mediated E2F1 SUMOylation. Bacterially expressed His-E2F1 were incubated with recombinant E1, E2, SUMO1 (WT or mutant), and His-Pc2 (unmethylated or methylated) in the presence of synthesized sense or antisense *TUG1* or *NEAT2* RNA oligos. The reactions were subjected to immunoblotting using antibodies against E2F1.
See also Figure S6.

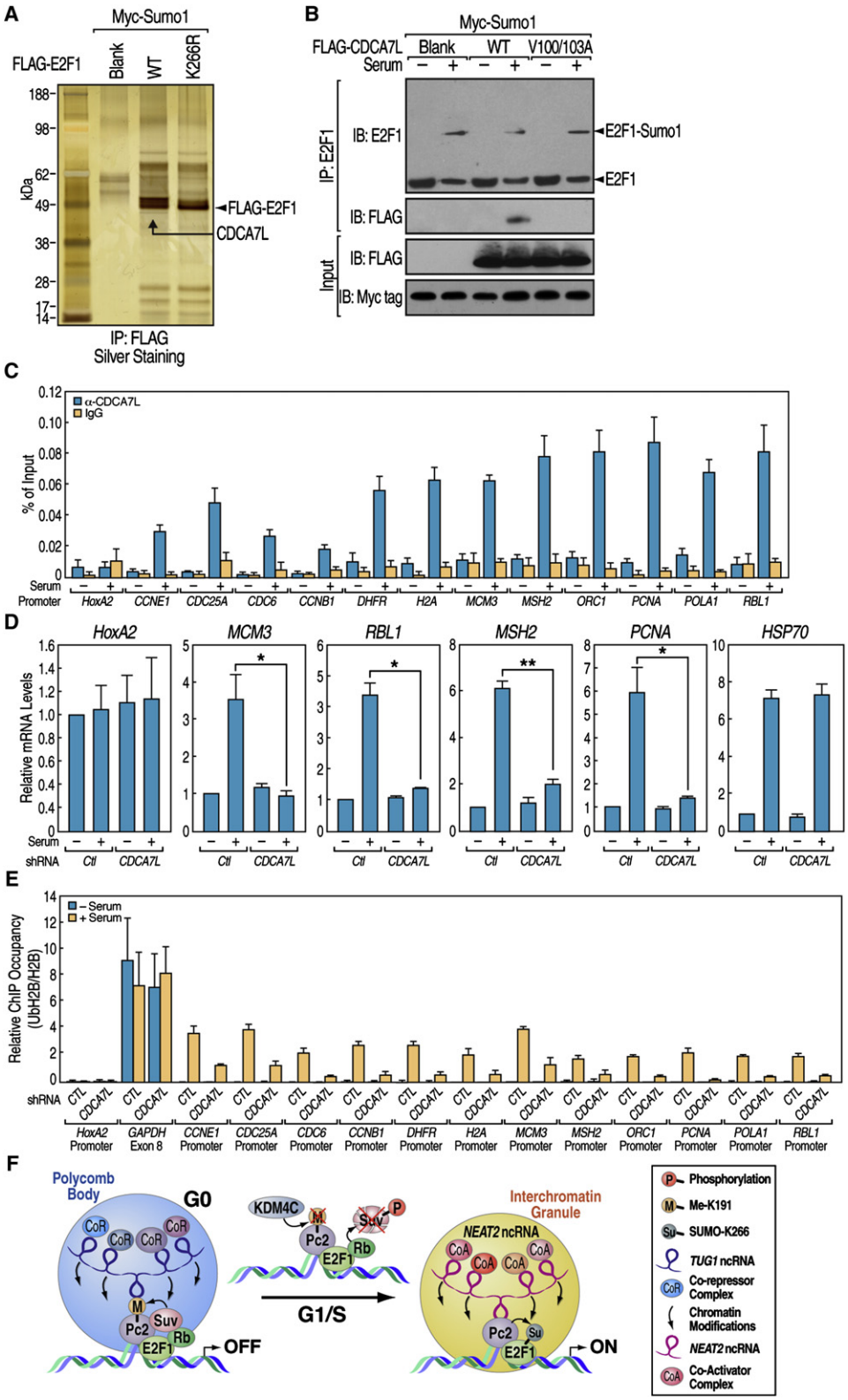

Figure 7. CDCA7L Interacts with SUMOylated E2F1 and Functions as a H2B Monoubiquitinase to Promote Growth-Control Gene Activation

(A) CDCA7L interacts with K266-SUMOylated E2F1. FLAG-E2F1 immunoprecipitates from HeLa cells were separated by SDS-PAGE followed by silver staining. The band indicated was cut and subjected to MS analysis.

Bagchi, S., Weinmann, R., and Raychaudhuri, P. (1991). The retinoblastoma protein copurifies with E2F-I, an E1A-regulated inhibitor of the transcription factor E2F. Cell *65*, 1063–1072.

Bernstein, E., Duncan, E.M., Masui, O., Gil, J., Heard, E., and Allis, C.D. (2006). Mouse polycomb proteins bind differentially to methylated histone H3 and RNA and are enriched in facultative heterochromatin. Mol. Cell. Biol. *26*, 2560–2569.

Bond, C.S., and Fox, A.H. (2009). Paraspeckles: nuclear bodies built on long noncoding RNA. J. Cell Biol. *186*, 637–644.

Campanero, M.R., and Flemington, E.K. (1997). Regulation of E2F through ubiquitin-proteasome-dependent degradation: stabilization by the pRB tumor suppressor protein. Proc. Natl. Acad. Sci. USA *94*, 2221–2226.

Chuikov, S., Kurash, J.K., Wilson, J.R., Xiao, B., Justin, N., Ivanov, G.S., McKinney, K., Tempst, P., Prives, C., Gamblin, S.J., et al. (2004). Regulation of p53 activity through lysine methylation. Nature *432*, 353–360.

Clemson, C.M., Hutchinson, J.N., Sara, S.A., Ensminger, A.W., Fox, A.H., Chess, A., and Lawrence, J.B. (2009). An architectural role for a nuclear noncoding RNA: NEAT1 RNA is essential for the structure of paraspeckles. Mol. Cell *33*, 717–726.

Cloos, P.A., Christensen, J., Agger, K., Maiolica, A., Rappsilber, J., Antal, T., Hansen, K.H., and Helin, K. (2006). The putative oncogene GASC1 demethylates tri- and dimethylated lysine 9 on histone H3. Nature *442*, 307–311.

Czvitkovich, S., Sauer, S., Peters, A.H., Deiner, E., Wolf, A., Laible, G., Opravil, S., Beug, H., and Jenuwein, T. (2001). Over-expression of the SUV39H1 histone methyltransferase induces altered proliferation and differentiation in transgenic mice. Mech. Dev. *107*, 141–153.

de la Luna, S., Burden, M.J., Lee, C.W., and La Thangue, N.B. (1996). Nuclear accumulation of the E2F heterodimer regulated by subunit composition and alternative splicing of a nuclear localization signal. J. Cell Sci. *109*, 2443–2452.

Deshaies, R.J., and Joazeiro, C.A. (2009). RING domain E3 ubiquitin ligases. Annu. Rev. Biochem. *78*, 399–434.

Eddy, S.R. (2001). Non-coding RNA genes and the modern RNA world. Nat. Rev. Genet. *2*, 919–929.

Fodor, B.D., Kubicek, S., Yonezawa, M., O'Sullivan, R.J., Sengupta, R., Perez-Burgos, L., Opravil, S., Mechtler, K., Schotta, G., and Jenuwein, T. (2006). Jmjd2b antagonizes H3K9 trimethylation at pericentric heterochromatin in mammalian cells. Genes Dev. *20*, 1557–1562.

Fu, X.D., and Maniatis, T. (1990). Factor required for mammalian spliceosome assembly is localized to discrete regions in the nucleus. Nature *343*, 437–441.

Hernández-Muñoz, I., Taghavi, P., Kuijl, C., Neefjes, J., and van Lohuizen, M. (2005). Association of BMI1 with polycomb bodies is dynamic and requires PRC2/EZH2 and the maintenance DNA methyltransferase DNMT1. Mol. Cell. Biol. *25*, 11047–11058.

Hu, Q., Kwon, Y.S., Nunez, E., Cardamone, M.D., Hutt, K.R., Ohgi, K.A., Garcia-Bassets, I., Rose, D.W., Glass, C.K., Rosenfeld, M.G., and Fu, X.D. (2008). Enhancing nuclear receptor-induced transcription requires nuclear motor and LSD1-dependent gene networking in interchromatin granules. Proc. Natl. Acad. Sci. USA *105*, 19199–19204.

Huang, A., Ho, C.S., Ponzielli, R., Barsyte-Lovejoy, D., Bouffet, E., Picard, D., Hawkins, C.E., and Penn, L.Z. (2005). Identification of a novel c-Myc protein interactor, JPO2, with transforming activity in medulloblastoma cells. Cancer Res. *65*, 5607–5619.

Huang, J., and Berger, S.L. (2008). The emerging field of dynamic lysine methylation of non-histone proteins. Curr. Opin. Genet. Dev. *18*, 152–158.

Huang, W., Ghisletti, S., Saijo, K., Gandhi, M., Aouadi, M., Tesz, G.J., Zhang, D.X., Yao, J., Czech, M.P., Goode, B.L., et al. (2011). Coronin 2A mediates actin-dependent de-repression of inflammatory response genes. Nature *470*, 414–418.

Hutchinson, J.N., Ensminger, A.W., Clemson, C.M., Lynch, C.R., Lawrence, J.B., and Chess, A. (2007). A screen for nuclear transcripts identifies two linked noncoding RNAs associated with SC35 splicing domains. BMC Genomics *8*, 39.

Jenuwein, T., and Allis, C.D. (2001). Translating the histone code. Science *293*, 1074–1080.

Kerscher, O. (2007). SUMO junction-what's your function? New insights through SUMO-interacting motifs. EMBO Rep. *8*, 550–555.

Khalil, A.M., Guttman, M., Huarte, M., Garber, M., Raj, A., Rivea Morales, D., Thomas, K., Presser, A., Bernstein, B.E., van Oudenaarden, A., et al. (2009). Many human large intergenic noncoding RNAs associate with chromatin-modifying complexes and affect gene expression. Proc. Natl. Acad. Sci. USA *106*, 11667–11672.

Kouzarides, T. (2007). Chromatin modifications and their function. Cell *128*, 693–705.

Lachner, M., O'Carroll, D., Rea, S., Mechtler, K., and Jenuwein, T. (2001). Methylation of histone H3 lysine 9 creates a binding site for HP1 proteins. Nature *410*, 116–120.

Lavrov, S., Déjardin, J., and Cavalli, G. (2004). Combined immunostaining and FISH analysis of polytene chromosomes. Methods Mol. Biol. *247*, 289–303.

Liu, W., Tanasa, B., Tyurina, O.V., Zhou, T.Y., Gassmann, R., Liu, W.T., Ohgi, K.A., Benner, C., Garcia-Bassets, I., Aggarwal, A.K., et al. (2010). PHF8 mediates histone H4 lysine 20 demethylation events involved in cell cycle progression. Nature *466*, 508–512.

Lund, A.H., and van Lohuizen, M. (2004). Polycomb complexes and silencing mechanisms. Curr. Opin. Cell Biol. *16*, 239–246.

Mercer, T.R., Dinger, M.E., and Mattick, J.S. (2009). Long non-coding RNAs: insights into functions. Nat. Rev. Genet. *10*, 155–159.

Minsky, N., Shema, E., Field, Y., Schuster, M., Segal, E., and Oren, M. (2008). Monoubiquitinated H2B is associated with the transcribed region of highly expressed genes in human cells. Nat. Cell Biol. *10*, 483–488.

Misteli, T. (2010). Higher-order genome organization in human disease. Cold Spring Harb. Perspect. Biol. *2*, a000794.

Nahle, Z., Polakoff, J., Davuluri, R.V., McCurrach, M.E., Jacobson, M.D., Narita, M., Zhang, M.Q., Lazebnik, Y., Bar-Sagi, D., and Lowe, S.W. (2002). Direct coupling of the cell cycle and cell death machinery by E2F. Nat. Cell Biol. *4*, 859–864.

Nevins, J.R. (1992). Transcriptional regulation. A closer look at E2F. Nature *358*, 375–376.

(B) CDCA7L interacts with SUMOylated E2F1 via its SUMO-interacting motif. HeLa cells transfected with indicated plasmids were serum-starved followed by restimulation, and the cells lysates were immunoprecipitated with E2F1 antibodies followed by immunoblotting with antibodies indicated.
(C) Serum-induced recruitment of CDCA7L on growth-control gene promoters. ChIP analyses were performed in serum-starved and restimulated HeLa cells using CDCA7L antibodies on indicated regions.
(D) CDCA7L is required for growth-control gene activation. HeLa cells transfected with shRNA against *CDCA7L* were serum-starved followed by restimulation, and relative mRNA levels of indicated genes were determined by qRT-PCR. Mean ± SEM, $^{*}p < 0.05$ and $^{**}p < 0.01$.
(E) CDCA7L is required for serum-induced histone H2B ubiquitination on growth-control gene promoters. HeLa cells transfected with shRNA against *CDCA7L* were serum-starved followed by restimulation, and ChIP analyses were performed using antibodies targeting UbH2B and H2B on indicated regions. For each primer pair, UbH2B values were normalized to the corresponding total H2B ChIP.
(F) Model: Interplay between ncRNAs and methylated versus unmethylated Pc2 determines intranuclear localization of growth-control genes in PcG bodies or ICGs, which dictates gene repression versus activation events.
See also Figure S7.

Nielsen, S.J., Schneider, R., Bauer, U.M., Bannister, A.J., Morrison, A., O'Carroll, D., Firestein, R., Cleary, M., Jenuwein, T., Herrera, R.E., and Kouzarides, T. (2001). Rb targets histone H3 methylation and HP1 to promoters. Nature *412*, 561–565.

Peters, A.H., O'Carroll, D., Scherthan, H., Mechtler, K., Sauer, S., Schöfer, C., Weipoltshammer, K., Pagani, M., Lachner, M., Kohlmaier, A., et al. (2001). Loss of the Suv39h histone methyltransferases impairs mammalian heterochromatin and genome stability. Cell *107*, 323–337.

Ponting, C.P., Oliver, P.L., and Reik, W. (2009). Evolution and functions of long noncoding RNAs. Cell *136*, 629–641.

Qi, H.H., Sarkissian, M., Hu, G.Q., Wang, Z., Bhattacharjee, A., Gordon, D.B., Gonzales, M., Lan, F., Ongusaha, P.P., Huarte, M., et al. (2010). Histone H4K20/H3K9 demethylase PHF8 regulates zebrafish brain and craniofacial development. Nature *466*, 503–507.

Rea, S., Eisenhaber, F., O'Carroll, D., Strahl, B.D., Sun, Z.W., Schmid, M., Opravil, S., Mechtler, K., Ponting, C.P., Allis, C.D., and Jenuwein, T. (2000). Regulation of chromatin structure by site-specific histone H3 methyltransferases. Nature *406*, 593–599.

Sampath, S.C., Marazzi, I., Yap, K.L., Sampath, S.C., Krutchinsky, A.N., Mecklenbräuker, I., Viale, A., Rudensky, E., Zhou, M.M., Chait, B.T., and Tarakhovsky, A. (2007). Methylation of a histone mimic within the histone methyltransferase G9a regulates protein complex assembly. Mol. Cell *27*, 596–608.

Satijn, D.P., Olson, D.J., van der Vlag, J., Hamer, K.M., Lambrechts, C., Masselink, H., Gunster, M.J., Sewalt, R.G., van Driel, R., and Otte, A.P. (1997). Interference with the expression of a novel human polycomb protein, hPc2, results in cellular transformation and apoptosis. Mol. Cell. Biol. *17*, 6076–6086.

Sewalt, R.G., Lachner, M., Vargas, M., Hamer, K.M., den Blaauwen, J.L., Hendrix, T., Melcher, M., Schweizer, D., Jenuwein, T., and Otte, A.P. (2002). Selective interactions between vertebrate polycomb homologs and the SUV39H1 histone lysine methyltransferase suggest that histone H3-K9 methylation contributes to chromosomal targeting of Polycomb group proteins. Mol. Cell. Biol. *22*, 5539–5553.

Simon, J.A., and Kingston, R.E. (2009). Mechanisms of polycomb gene silencing: knowns and unknowns. Nat. Rev. Mol. Cell Biol. *10*, 697–708.

Subramanian, K., Jia, D., Kapoor-Vazirani, P., Powell, D.R., Collins, R.E., Sharma, D., Peng, J., Cheng, X., and Vertino, P.M. (2008). Regulation of estrogen receptor alpha by the SET7 lysine methyltransferase. Mol. Cell *30*, 336–347.

Szczerbal, I., and Bridger, J.M. (2010). Association of adipogenic genes with SC-35 domains during porcine adipogenesis. Chromosome Res. *18*, 887–895.

Ule, J., Jensen, K., Mele, A., and Darnell, R.B. (2005). CLIP: a method for identifying protein-RNA interaction sites in living cells. Methods *37*, 376–386.

Wilusz, J.E., Sunwoo, H., and Spector, D.L. (2009). Long noncoding RNAs: functional surprises from the RNA world. Genes Dev. *23*, 1494–1504.

Xu, X., Hoang, S., Mayo, M.W., and Bekiranov, S. (2010). Application of machine learning methods to histone methylation ChIP-Seq data reveals H4R3me2 globally represses gene expression. BMC Bioinformatics *11*, 396.

Yamane, K., Toumazou, C., Tsukada, Y., Erdjument-Bromage, H., Tempst, P., Wong, J., and Zhang, Y. (2006). JHDM2A, a JmjC-containing H3K9 demethylase, facilitates transcription activation by androgen receptor. Cell *125*, 483–495.